PHYSICAL REVIEW C VOLUME 40, NUMBER 5 NOVEMBER 1989

Two statistical approaches to nuclear disassembly

William A. Friedman*
Physics Department, University of Wisconsin, Madison, Wisconsin 53706
and Bereich Physik, Hahn-Meitner-Institut, D-1000 Berlin 39, Germany
(Received 5 June 1989)

Two statistical approaches to nuclear disassembly are compared. One is based on a sequential chain of binary decays, and the other on the microcanonical treatment of fragment configurations in a fixed freeze-out volume. The two approaches are formulated in a manner to facilitate this comparison. A volume related to the sequential approach is defined. This volume is interpreted in terms of entropy conservation. Effective freeze-out volumes are defined for various yields. From this it is shown how similar predictions can arise from the approaches which are based on mutually incompatible assumptions. Differences in Coulomb effects are explored. A detailed comparison of two sets of predictions is made for a test example, and the reasons behind specific differences are studied. It is suggested that such differences can serve as experimental signatures to distinguish which approach is more appropriate.

I. INTRODUCTION

Two different theoretical procedures both based on phase-space statistical features are currently being used to calculate the yields of intermediate mass fragments from highly excited nuclei. These procedures are very different in their, assumptions, input parameters, and supposed scenarios for the formation of the fragments.

One of these, exemplified by the calculations of Ref. 1, treats a decaying source which deexcites by a series of binary decays wherein a fragment (relatively unexcited) separates from the larger excited source. This procedure assumes that the total breakup follows from a chain of sequential binary processes. In the following discussion this procedure will be designated as the *sequential* approach. The total inclusive yield of the fragments calculated by this procedure is determined by summing the contributions from each of the individual decays which occur during the cooling process. The rates at each stage are calculated, and branching ratios, obtained from these, determine the competition among the different channels for decay at each stage. The relative decay rates are calculated using the assumption of detailed balance proposed by Weisskopf.[2] This leads to rates which are governed, in part, by the relative phase space for each of the possible binary processes. The detailed-balance procedure requires one to calculate the rate for the inverse reaction, i.e., absorption. It is in combination with this inverse rate that phase space (density of states) determines the emission rate.

The other approach, exemplified by the calculations of Ref. 3, takes a microcanonical approach. It assumes that the yield of fragments is determined by the relative phase-space weights (density of states) for channels chosen in a given volume (freeze-out volume) at one instant. This approach will be designated hereafter as the *freeze-out* approach. The phase-space considerations in this procedure involve distributions which have numerous fragments—not simply the binary pairs involved at each stage of a sequential breakup. It is assumed that all of the particles are in equilibrium with one another in the freeze-out volume, that each configuration is equally likely, and that the distribution among the particles is fixed as the system expands beyond the freeze-out volume. A crucial element, or parameter, of all calculations based on this procedure is the specific size of the freeze-out volume.

In the freeze-out approach the entropy increases up to the freeze-out condition and remains constant thereafter. On the other hand in the sequential decay approach the entropy is determined at the initial decay stage prior to emission.

Both procedures have been applied to excited systems which ultimately result in tens of fragments. The assumption, at lower energies, that there exists a single freeze-out volume or a time at which all the fragments are in equilibrium, seems highly questionable. On the other hand, at higher energies where successive steps follow closely on one another, the assumption that the steps are distinct also becomes questionable. Calculations using both of these techniques have been carried out over wide ranges of energy, where one might expect one or the other of these procedures to be invalid. The surprising feature of these calculations is that they provide inclusive particle yields which are qualitatively similar despite the great qualitative difference in the assumptions underlying each of the procedures.

The purpose of this work is to explore the relationship between the two procedures. By so doing we will demonstrate how both procedures can provide similar values for inclusive yields even when their assumptions are complementary. One of the difficulties in comparing the two approaches is that the sequential approach is framed in terms of instantaneous rates, which change as the residue cools, while the full phase-space procedure is framed in terms of probabilities. In addition, the freeze-out volume, which is crucial to the results of the full phase-space approach never enters the sequential picture, while

the cross section and flux for the absorption process, which are important to the latter, play no role in the full phase-space approach.

In Sec. II we review the formal structure of the two approaches and establish the notation followed in the remainder of the paper. We reformulate the sequential approach in terms of probabilities by using the rates to obtain branching ratios. Probabilities for given configurations of fragments can be obtained from these ratios. We then express the relative probability weights for a given configuration, in the language of each of the approaches. This exercise is used to illustrate the formal (structural) connection between the freeze-out volume, on the one hand, and the product of factors in the sequential approach which constitute an *effective* volume.

In Sec. III we interpret the *effective* volume of Sec. II in terms of entropy conservation. This will also demonstrate that total entropy is conserved with each emission ever though the entropy of the residue decreases.

Section IV deals with a formal comparison of the volume aspects of the two approaches. We obtain *equivalent* freeze-out volumes, which, when used in the full phase-space formalism, can reproduce the multiplicities predicted by the sequential approach. We consider a specific case of ^{197}Au to examine these equivalent volumes at different excitation energies. This illustration provides a means of seeing why the similar numerical predictions arise from the disparate and mutually incompatible approaches.

In Sec. V we discuss those differences between the two approaches which arise from differences in the way each deals with the Coulomb effects. In Sec. VI we predict various features for the disassembly of a given test system using two formalisms based on the two approaches. We note the differences and show how these can be understood in terms of the discussions of the previous sections. The differences which are found suggest signatures for determining which approach is most appropriate for a given experimental situation. Section VII contains a brief summary of conclusions.

II. FORMALISM

IN this section we develop formal expressions that are useful in calculating the relative probability for the disassembly of an excited nucleus into various groups of fragments. These will be developed for both the sequential and the freeze-out procedures. Our purpose is to establish a notation for later discussions and also to provide expressions for each of the two approaches which may be compared most easily.

A. Sequential approach

We begin by considering one stage in the sequential decay. Let us consider an excited system C_1, which decays into a residue C_2, plus an emitted particle labeled b. The general expression for the rate of this decay is given by

$$(dN_b/dt)_{\text{emission}}=(2\pi/\hbar)|M_{if}|^2\rho_f \ , \tag{2.1}$$

where i represents a compound nuclear state C_1, with energy E_i, and f represents the products of the decay, i.e., the residue and emitted particle. The density of final states is represented by ρ_f. The matrix element $|M_{if}|$ can be estimated under the assumption of detailed balance as suggested by Weisskopf.[2] For this we consider the inverse process, absorption, for which

$$(dN_b/dt)_{\text{absorption}}=\sigma_{b+C_2}\phi_b$$
$$=(2\pi/\hbar)|M_{fi}|^2\rho_i \ , \tag{2.2}$$

where σ is the absorption cross section and ϕ is the incoming flux of particles b. The states represented by i and f are the same as above. If we assume that the magnitude of the two matrix elements are equal, then

$$(dN_b/dt)_{\text{emission}}=(\sigma_{b+C_2}\phi_b)(\rho_f/\rho_i) \ . \tag{2.3}$$

Following Weisskopf, we next take the flux as that associated with a single particle in an very large box of volume Ω. This provides a flux, $\phi=v/\Omega$, where v is the velocity of the emitted particle. The level density $\rho_i(E_i)$ is the density of the microscopic states of the excited system C_1. For ρ_b we use the following expression treating the continuum states in a semiclassical fashion:

$$\rho_f=\int\rho_{C_2}[E_i-p_b^2/(2m_b)-S_b]g_b d^3p_b\Omega/(2\pi\hbar)^3 \ , \tag{2.4}$$

where ρ_{C_2} is the density of the microscopic states of the residual system C_2 following emission of particle b which has mass m_b, separation energy S_b, and degeneracy g_b. We assume a simple geometric form for the absorption cross section,

$$\sigma_{b+C_2}=\sigma_{\text{geo}}(b,C_2)[1-V^{\text{Coul}}(b,C_2)/E_b]$$
$$\times\Theta[1-V^{\text{Coul}}(b,C_2)/E_b] \ , \tag{2.5}$$

where $\sigma_{\text{geo}}=\pi R^2$ and V^{Coul} is the Coulomb barrier.

We combine these expressions into Eq. (2.3) and shift the energy scale for the emitted particles so that the new momentum $\tilde{p}$ is given by

$$\tilde{p}^2/(2m_b)=p^2/(2m_b)-V^{\text{Coul}} \ . \tag{2.6}$$

This leads to the following expression for the emission rate:

$$(dN_b/dt)=\int \sigma_{\rm geo}(b,C_2)\bar{v}_b\rho_{C_2}[E_i-\tilde{p}^2/(2m_b)-V^{\rm Coul}-S_b]/\rho_{C_1}(E_i)g_b d^3\tilde{p}/(2\pi\hbar)^3 \ . \tag{2.7}$$

This integral extends over the entire space of momentum since $\tilde{p}$ goes to zero at the top of the Coulomb barrier. In subsequent expressions we drop the tilde from v and p but the meaning is unchanged.

We now use the expressions for the decay rate to obtain the branching ratios, $R_b(C)$. These give the probability that the decay, which occurs from condition C, results in the emission of particle b:

$$R_b(C)=\Gamma_b/\Gamma=[dN_b(C)/dt]\Big/\sum_{b'}(dN_{b'}/dt) \ . \tag{2.8}$$

The branching ratio can be written in the following form:

$$R_b(C)=\int g_b d^3p/(2\pi\hbar)^3 B(b,\mathbf{p};C,E_C) \ , \tag{2.9}$$

where

$$B(b,\mathbf{p};C_1,E_1)=[\sigma_{\rm geo}(b,C_2)v_b\tau(C_1)]\rho_{C_2}[E_{C_1}-p_b^2/(2m_b)-S_b-V^{\rm Coul}(b,C_2)]/\rho_{C_1}(E_{C_1}) \ , \tag{2.10}$$

where C_2 is the residue of the decay of C_1 by the emission of particle b and $\tau=\hbar/\Gamma$.

Let us now consider the decay of the system C_1 by a chain of N sequential decays into specific fragments, b_i $(i=1\rightarrow N)$ and a final residue C_{N+1}. The probability weight for the emission of this set of fragments, $W(\{b_i\})$, is found from a product of probabilities associated with each stage of the decay

$$W(\{b_i\})=\sum_{\rm permut}\int\prod_{i=1}^{N}B(b_i,\mathbf{p}_i,C_i,E_i)(g_b d^3p_{b_i}/(2\pi\hbar)^3\prod_{i=2}^{N}dC_{i+1}\delta[C_{i+1},(C_i-b_i)] \ , \tag{2.11}$$

where the symbolic δ function in the integral over C_{i+1} signifies that the mass, charge, and energy of the residue, be found from C_i by the removal of particle b_i, for example,

$$E_{C_{i+1}}=E_{C_i}-p_{b_i}^2/(2m_{b_i})-S_{b_iC_i}-V^{\rm Coul}_{b_i,C_{i+1}} \ . \tag{2.12}$$

The chain of factors $\rho_{C_{i+1}}/\rho_{C_i}$, which implicitly occurs in Eq. (2.11) in the product of $B(b_i,\mathbf{p}_i;C_i,E_i)$, simplifies by pairwise cancellation so that

$$W(\{b_i\})=\sum_{\rm permut}\int\prod_{i=1}^{N}(g_{b_i}d^3p_{b_i}/(2\pi\hbar)^3(\sigma v\tau)_i(\rho_{C_{N+1}}/\rho_{C_1})\prod_{i=2}^{N}\delta[C_{i+1},(C_i-b_i)]dC_{i+1} \tag{2.13}$$

with

$$(\sigma v\tau)_i\equiv[\sigma_{\rm geo}(b_i,C_{i+1})v_{b_i}\tau(C_i)] \ .$$

The collection of fragments $\{b_i\}$ can be specified by the number n_α, of each type of fragment α. We then note that the sum over the permutations of emission order involves $N!/\prod n_\alpha!$ terms.

Finally we can use the probability information for each chain of decays to obtain a prediction of the mean multiplicity, m_α, for specific type of fragment. It has been shown in Ref. 4 that the mean multiplicity can be found by summing the probability for production at each stage. This is given by

$$m_\alpha=\sum_{\rm stages}\langle R_\alpha(C_i)\rangle \ , \tag{2.14}$$

where the angular brackets represent an average over all the conditions C_i encountered in the collection of all possible chains. Finally, it was shown in Ref. 4 that an approximate value of the multiplicity is obtained from

$$m_\alpha\approx\sum R_\alpha(\langle C_i\rangle) \ , \tag{2.15}$$

where the average values of the conditions for each stage are used.

B. Freeze-out approach

We now turn to the freeze-out procedure for determining fragment yields. As in the previous subsection, let us consider the break up of a system C_1 into N fragments, $b_1,b_2,\ldots,b_N$, plus a residue C_{N+1}. The collection of fragments is characterized by n_α, which gives the number of fragments of the type α among the collection.

We next determine the relative probability for the chosen emission configuration. In the freeze-out picture this probability is proportional to the density of final states in the freeze-out volume of chosen size

$$\rho_f \propto \int \prod_{i=1}^{N} g_{b_i} d^3p_{b_i} d^3r_{b_i}/(2\pi\hbar)^3 \rho_{C_{N+1}}(E_{C_{N+1}}) \delta\left\{E_{C_{N+1}} - \left[E_{C_1} - \sum p_{b_i}^2/(2m_{b_i}) - \sum S_{b_i} - V^{\text{Coul}}\right]\right\} \Big/ \left[\prod n_\alpha!\right] . \quad (2.16)$$

In the expression above the spacial integral is taken over the freeze-out volume. If this volume is not too small the excluded volume (avoided overlap) can be ignored and we may approximate each of the integrals over spacial coordinates by the full freeze-out volume V_F and replace the Coulomb potential energy V^{Coul} in the energy conserving δ function by its average. Equation (2.16) involves a *relative* probability. This is unchanged if we multiply by a factor common to all final configurations, namely, $1/\rho_{C_1}(E_1)$:

$$\rho_f \propto \left[N! \Big/ \prod n_\alpha!\right](V_F^N/N!) \int \prod_{i=1}^{N} g_{b_i} d^3p_{b_i}/(2\pi\hbar)^3 [\rho_{C_{N+1}}(E_{C_{N+1}})/\rho_{C_1}(E_{C_1})] \times \delta\left\{E_{C_{N+1}} - \left[E_{C_1} - \sum p_{b_i}^2/(2m_{b_i}) - \sum S_{b_i} - V^{\text{Coul}}\right]\right\} . \quad (2.17)$$

Next let us consider the permutations of the order of factors in the product over fragments. We can replace the factor $(N!/\prod n_\alpha!)$ by a sum over all such permutations. Finally, for each permutation, let us introduce unity in the following representation:

$$1 = \rho_{C_2}(\rho_{C_3}/\rho_{C_2})(\rho_{C_4}/\rho_{C_3}) \ldots (1/\rho_{C_N}) , \quad (2.18)$$

where the C_i's and E_{C_i}'s are chosen consistent with the b_i's for a given permutation.

Let us represent the average Coulomb energy by a multiple of the sum of pairwise Coulomb barriers used in the sequential decay

$$\langle V^{\text{Coul}} \rangle \approx f \sum V^{\text{Coul}}(b_i, C_{i+1}) . \quad (2.19)$$

The factor f suggests that the Coulomb energy associated with the freeze-out configuration differs from the simple sum of Coulomb barriers. In the latter, particles leaving the residue with zero relative velocity acquire kinetic energy as they move outward from the barrier tops. This kinetic energy represents the total Coulomb energy associated with the sequential picture. In the freeze-out picture, on the other hand, the particles once released remain in equilibrium with the other fragments in the freeze-out volume. Those particles with zero velocity at the freeze-out configuration subsequently acquire kinetic energy in moving from that configuration to infinity. On average the electrical potential energy of the charged fragments is lower in the freeze-out configuration than at the top of the barriers of the residues. For this reason one would expect the factor f in Eq. (2.19) to be less than 1.

With the Coulomb energy represented by the sum in Eq. (2.19) we may now write the energy conserving δ function of Eq. (2.17) as follows:

$$\delta\left\{E_{C_{N+1}} - \left[E_{C_1} - \sum p_{b_i}^2/(2m_{b_i}) - \sum S_{b_i} - V^{\text{Coul}}\right]\right\} = \int \prod_{i=2}^{N} dC_{i+1} \delta\{E_{C_{i+1}} - [E_{C_i} - p_{b_i}^2/(2m_{b_i}) - S_{b_i} - fV^{\text{Coul}}(b_i, C_{i+1})]\} . \quad (2.20)$$

Combining the features above, we obtain an expression for the relative weight given the chosen configuration in the freeze-out picture, which can readily be compared with the corresponding weight given in the sequential picture

$$W(\{b_i\}) \propto \rho_f \propto \sum_{\text{permut}} \int \prod_{i=1}^{N} g_{b_i} d^3p_{b_i}/(2\pi\hbar)^3 (eV_F/N)(\rho_{C_{N+1}}/\rho_{C_1}) \prod_{i=2}^{N} \delta[C_{i+1}, (C_i - b_i)] dC_{i+1} , \quad (2.21)$$

where we have used Stirling's approximation, $N! \approx (N/e)^N$.

Let us compare Eq. (2.13) in the sequential approach with Eq. (2.21) in the freeze-out approach. The factors which are common to the two expressions have the same meanings with the exception of the relationship between $E_{C_{i+1}}$ and E_{C_i}. In the freeze-out picture this involves a modified Coulomb barrier height. Apart from this difference, to which we will return in Sec. V, it can clearly be seen that probability weights for a given configuration calculated in a freeze-out picture and those in a sequential decay picture involve expressions where the factor (eV_F/N) of the former is replaced by $(\sigma v \tau)_i$ of the latter.

While (eV_F/N) is a constant for a given decay, $(\sigma v \tau)_i$ depends both on the type of emitted fragment through σ and v and on the stage of emission i through τ. Whereas in the freeze-out approach, the coordinate volume is mutually occupied by all the fragments, in the sequential decay picture a phase-space volume can be assigned to each of the fragments individually. The coordinate portions of these volumes are not common to all the fragments. In

stead, the fragments occupy mutually exclusive zones at different distances from the center of decay. The phase-space volume for each decay fragment is determined during the stage of its decay and then the magnitude of this volume remains constant for subsequent times as the fragment moves away and another is emitted. The topic of volumes in the sequential decay picture is investigated and interpreted in the following section.

III. VOLUMES AND ENTROPY CONSIDERATIONS

In this section we examine that factor which is substituted for the freeze-out volume in the sequential approach. We shall provide a physical interpretation of this factor and show that it is related to the conservation of entropy in the emission process.

Let us first consider a specific binary decay

$$C_1 \rightarrow C_2 + b \ , \tag{3.1}$$

where the system C_1 has energy E_1. Let us assume that after emission the particle b is confined to a volume V. If the entropy before and after decay is to be the same then a specific value of V is required. This will be called the *isentropic* volume. This volume is determined by

$$e^{S_{C_1}(E_1)} = \int e^{S_{C_2}(E_1 - p_b^2/(2m_b) - S_b)} g_b d^3p_b/(2\pi\hbar)^3 V \ , \tag{3.2}$$

where S_b, g_b, and m_b are the separation energy, degeneracy factor, and the mass of the emitted fragment, and $S(E)$ represents the respective entropies of the systems C_1 and C_2. When we associate the density of states with the exponential of the entropy we obtain the following condition for the isentropic volume:

$$1 = \int \rho_{C_2}[E_1 - p_b^2/(2m_b) - S_b]/\rho_{C_1}(E_1) g_b d^3p_b/(2\pi\hbar)^3 V \ . \tag{3.3}$$

Let us now compare this condition with a similar condition which arises in the detailed-balance expression for the decay rate given in the preceding section:

$$(dN_b/dt) \equiv 1/\tau_b = \int (\sigma v)\rho_{C_2}[E_1 - p_b^2/(2m_b) - S_b]/\rho_{C_1}(E_1) g_b d^3p_b/(2\pi\hbar)^3 \ . \tag{3.4}$$

Upon rearrangement this becomes

$$1 = \int \langle \sigma v \tau_b \rangle \rho_{C_2}[E_1 - p_b^2/(2m_b) - S_b]/\rho_{C_1}(E_1) g_b d^3p_b/(2\pi\hbar)^3 \ , \tag{3.5}$$

where $\langle \sigma v \tau_b \rangle$ involves the average of $\mathbf{p}_b$ taken with weight given by (ρ_{C_2}/ρ_{C_1}).

Clearly $\langle \sigma v \tau_b \rangle$ can be associated with the *isentropic* volume. If we take $\sigma = \pi R^2$ then this is the volume that is occupied by the average flux which comes from the surface of the source during the period of time associated with the emission of one fragment of type b. As such, it expresses the uncertainty in location of that particle. Thus, it is reasonable that $\langle \sigma v \tau_b \rangle$ represent the volume portion of the phase space for the emitted particle.

As an illustration, let us apply the aforementioned conditions to the case of a free gas of A identical particles in a spherical volume of size $\tilde{V}$, from which the particles emerge without requiring separation energy. We can easily calculate the number of states before and after emission, and find the volume V in which the emitted particle must be confined in order to keep the entropy (number of states) constant.

The initial number of states is given by

$$\int \tilde{V}/A! \prod_{i=1}^{A} d^3p_i/(2\pi\hbar)^3 \delta\left[E_1 - \sum p_i^2/(2m)\right] \ . \tag{3.6}$$

If the final residue occupies the same volume as the initial system then the final number of states is given by

$$\int \tilde{V}^{A-1}/(A-1)! \prod_{i=1}^{A-1} d^3p_i/(2\pi\hbar)^3 \delta\left[E_1 - \sum^{A-1} p_i^2/(2m)\right] \delta\{E_2 - [E_1 - p_A^2/(2m)]\} dE_2 d^3p_A/(2\pi\hbar)^3 V \ . \tag{3.7}$$

The condition which conserves the entropy is

$$V = \tilde{V}/A \ . \tag{3.8a}$$

If the residue were to have the same density (as against the same volume) as the original system then the condition for constant entropy is

$$V \approx \tilde{V}e/A \ . \tag{3.8b}$$

The approximation indicated for this result is $(1 - 1/A)^{A-1} \approx 1/e$.

By reversing the preceding arguments one can use the isentropic volume to find the decay rate. For the simple example of a gas of identical particles in a sphere we obtain

$$\Gamma/\hbar = 1/\tau = \pi R^2 \langle v \rangle A/\tilde{V} = \tfrac{3}{4}\langle v \rangle A/R \ . \tag{3.9}$$

This corresponds to the result obtained by counting the instantaneous flow of particles through the walls of the sphere.

Let us next consider the competition among various

binary decay channels of a source. We assume that fragments of type b emerge into isentropic volumes V_b, and that the number of final states is obtained by summing over all of the types of emitted fragments. The requirement that entropy be conserved then becomes

$$1=\sum_b \int \rho_{C_1-b}/\rho_{C_1} g_b d^3p_b/(2\pi\hbar)^3(V_b) \ . \tag{3.10}$$

The full decay rate is the sum of the partial decay rates so that

$$1=\sum_b (\tau/\tau_b) \ , \tag{3.11}$$

where τ is the time for decay of the original system by any of the available channels. With the detailed-balance expression for τ_b we obtain

$$1=\sum_b \int \langle \sigma_b v_b \tau \rangle \rho_{C_1-b}/\rho_{C_1} g_b d^3p_b/(2\pi\hbar)^3 \ , \tag{3.12}$$

where the average is taken over the momentum distribution.

Comparing Eq. (3.12) and (3.10) we find that the isentropic volume V_b may be associated with $\langle \sigma_b v_b \tau \rangle$. This is the same "volume" expression that arose in the previous section.

IV. FORMAL COMPARISON OF APPROACHES: SIMILARITIES

In this section we make a formal comparison of predictions for fragment multiplicity according to the two procedures. We have previously noted that the freeze-out volume is a parameter to be chosen in that approach. In this section we will define an *effective* freeze-out volume which can be associated with each sequential decay calculation. We will show that the value of such a volume is, in many cases, not dissimilar from those volumes conventionally chosen in the freeze-out approach. The extent to which the two are the same suggests that multiplicity predictions can be similar using the two approaches.

In Sec. II we demonstrated that the structural difference between the freeze-out and the sequential predictions for the decay into M fragments is essentially associated with the replacement of $V_F e/M$ in the former by $\langle \sigma_b v_b \tau \rangle$ in the latter. Imagine that for every fragment b and every stage i that the two factors were identical. Then we would expect the multiplicities predicted by the two methods to be the same. In general, the factors are not the same. We now define the *effective* freeze-out volume for the sequential approach to be that volume which, used in the freeze-out approach, will provide the same multiplicity.

To obtain such a volume let us modify each of the branching ratios that appears in the sequential expressions for configuration probability by the following:

$$R_b(C_i) \rightarrow R_b(C_i) f_{i,b} \ , \tag{4.1}$$

where

$$f_{i,b} \equiv (V_{\text{eff}} e/M)/(\langle \sigma_b v_b \tau \rangle) \ . \tag{4.2}$$

This procedure has the effect of converting the sequential decay expression into a freeze-out expression with volume V_{eff}. The multiplicity for a specific fragment, α, is approximated in Eq. (2.15) by

$$m_\alpha = \sum_i R_\alpha(\langle C_i \rangle) \ .$$

To determine V_{eff} we require that the multiplicity remain unchanged by the modification of Eq. (4.1),

$$\sum_i R_\alpha(\langle C_i \rangle) f_{i,\alpha} = \sum_i R_\alpha(\langle C_i \rangle) \ . \tag{4.3}$$

This definition leads to the following value for V_{eff}:

$$V_{\text{eff}} = M/e\langle [1/(\langle \sigma_\alpha v_\alpha \rangle \tau)] \rangle \ , \tag{4.4}$$

where the inner average (as above) is over the velocity distribution of the fragments, and the outer average is over the stages of decay weighted according to the corresponding branching ratio.

The specific value of V_{eff} depends on both the fragment type α and the initial excitation energy. We shall illustrate this dependence through an example to follow.

It is useful for comparison to specify V_{eff} by an effective radius r_{eff} where $V_{\text{eff}} = 4\pi/3 r_{\text{eff}}^3 A$, with A the mass number of the original system. This permits easy comparison of the freeze-out density with that of nuclear matter for which a value of $r_{\text{eff}} \approx 1.1$ is appropriate. It also permits comparison with the range of the nuclear force.

As a specific example we consider a ^{197}Au nucleus which is excited to an initial temperature of 6 MeV (excitation of approximately 538 MeV). We have calculated the decay rates at successive stages using the formalism described in Ref. 1. We include 65 isotopes with mass number less than 20, and include bound states of these as fragments competing for emission. The calculation predicts a mean multiplicity of 28 fragments, most of which are neutrons. From these results we have calculated the decay time at each stage and the branching ratios. For the average over fragment cross section and velocity we have taken

$$\langle \sigma_b v_b \rangle_i = \pi r_0^2 (A_{C_i}^{1/3} + A_b^{1/3})^2 [8T_i/(\pi m_b)]^{1/2} \ , \tag{4.5}$$

where T_i is the temperature at stage i.

In Fig. 1 we display the results of the calculation of r_{eff} for a large number of isotopes whose mass is given along the abscissa. The general trend of the results is to suggest a value for the effective radius which is about 2 fm. This is roughly the value used in freeze-out calculations. It is clear, however, that the effective volume depends on the fragment type, and it varies in a systematic way, reducing with increasing mass. This dependence arises predominately from the fragment mass dependence in the average velocity. Since, for a given stage, the average kinetic energy of each fragment type is the same, the average velocity must go inversely as the square root of the mass. This follows the general trend in Fig. 1. This trend suggests that predictions by the sequential decay approach will suppress heavier fragments relative to light (or emphasize light relative to heavy) when compared to a

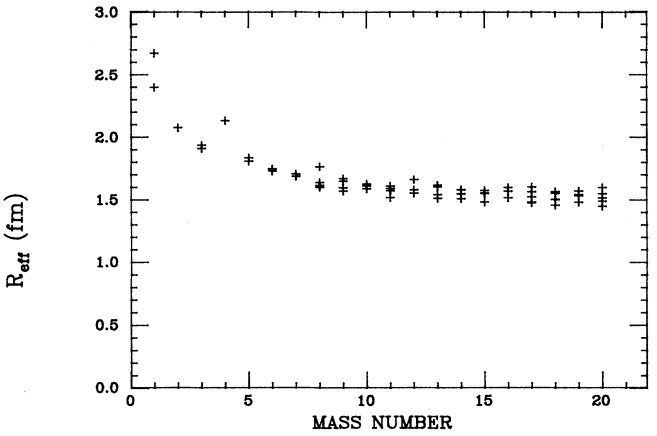

FIG. 1. Calculated effective freeze-out radii for the yield of various isotopes from ^{197}Au excited to 538 MeV.

freeze-out calculation which sets one volume for all types of particles.

We have multiplied each cross section by $(m_b)^{1/2}$ to effectively remove the mass dependence in the velocity. The subsequent values of r_{eff} are shown in Fig. 2. Note that some variation of r_{eff} with the fragment type remain. These variations result from differences in the profile of the branching ratio with the decay stage, and also from the weak dependence of the geometric cross section on fragment size. The values for both neutrons and α particles, whose emission continues to the latest stages, are higher than average. The sequential decay will emphasize neutron emission due to both the late decay and the low mass of this particle.

We find that the effective volume also depends on the initial excitation energy. To illustrate this dependence we have calculated, as a function of excitation energy, effective freeze-out volumes to provide the same multiplicity of (a) neutrons, (b) charged particle, (c) heavy particles (mass number greater than 8), and (d) total multiplicity. The four corresponding effective radii are plotted against excitation energy in Fig. 3. The effective volume tends to decrease with increasing excitation energy due primarily to decreasing decay times. The difference between neutrons and heavy fragments is greatest for the lower energies. The total multiplicity is to a great extent dominated by the neutron yield especially at the lowest energies. Let us assume that a freeze-out calculation is performed with radius of 2 fm. Then at the lowest energies we would expect close agreement between sequential decay and freeze-out predictions for heavy fragment emission. A large difference with respect to the lightest fragments would be expected, however, with the sequential approach predicting much higher yields. For energies of about 1 GeV, the neutron and total multiplicities would be similar but the charged particle and heavy fragments would be suppressed in the sequential approach relative to a freeze-out calculation.

The foregoing discussion only compares the numerical predictions that the two methods are likely to give and does not address the question of which of the two methods is more likely to be valid in different energy regimes. Clearly the assumptions of the freeze-out approach are not likely to be valid at low energies, and those of the sequential decay are not likely to be valid at the highest energies. In general the assumptions make the two approaches complementary. The results displayed in Fig. 3 suggest, however, that over a very wide range of energies some or all of the multiplicity predictions of the two methods may be numerically similar despite the vast differences in the assumptions of the two approaches. In Sec. VI we will concentrate on the differences in the predictions and discuss possible experimental signatures to distinguish which method is most appropriate.

V. COULOMB POTENTIAL ENERGY

In Sec. II we pointed out that in the freeze-out expression the total energy of a configuration requires the

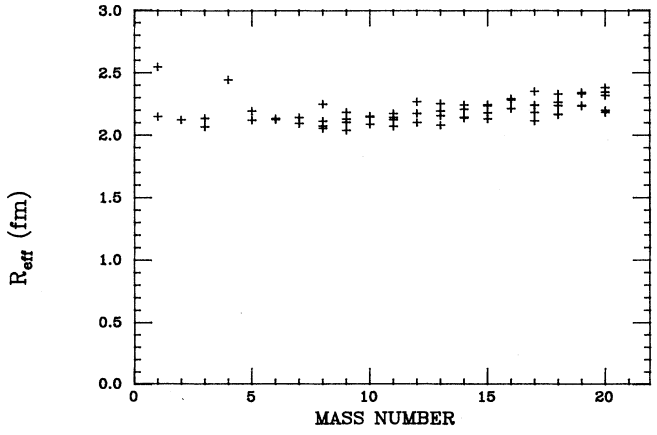

FIG. 2. Calculated effective freeze-out radii for the yield of various isotopes from ^{197}Au excited to 538 MeV. Each absorption cross section has been multiplied by the square root of the fragment mass to remove the mass effect from the velocity.

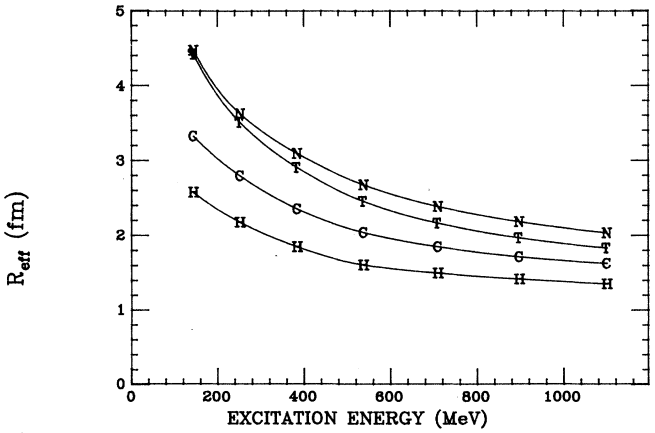

FIG. 3. Effective freeze-out radii as a function of initial excitation energy for the yield of neutrons (N), charged fragments (C), heavy fragments (H), and total multiplicity (T).

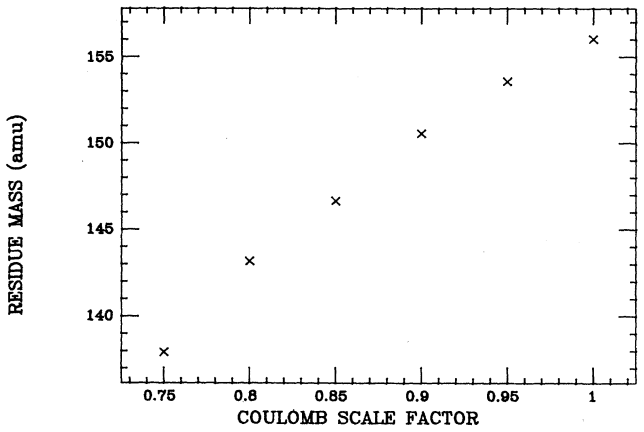

FIG. 4. Mass of final residue, from the decay of ^{197}Au excited to 538 MeV, as a function of the scale factor of the Coulomb barriers in sequential decay.

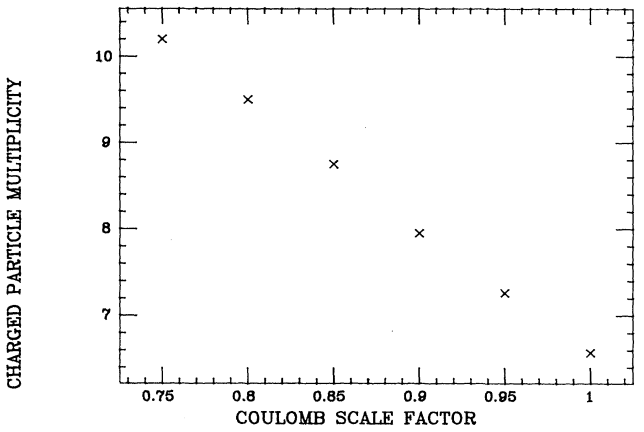

FIG. 6. Multiplicity of charged fragments, from the decay of ^{197}Au excited to 538 MeV, as a function of the scale factor for the Coulomb barriers in sequential decay.

many-body Coulomb potential for the fragmentation. A similar role is played in the sequential approach by the sum of binary Coulomb barriers for each of the stages of decay. This represents a major difference between the approaches. As we have noted, the many-body Coulomb potential energy in the freeze-out volume would be expected to be lower than the sum of barriers since the particles on average are farther apart. This effect can be examined by exploring sequential decay calculations with reduced Coulomb barriers at each of the binary decays. This was suggested in Eq. (2.19) where we introduced the scale factor f in each of the energy conserving delta functions. We will examine how reduced barriers influence several aspects of the multiplicity yields. Some of these features may permit discrimination between experimental situations in which either sequential decay or freeze out occurs.

The mass of the mean residue at the end of the decay is found to be strongly influenced by the magnitude of the Coulomb barrier. We have used sequential decay calculations with Coulomb barriers reduced by scaling factors to obtain predictions of the mass of final residues. The initial system is ^{197}Au discussed in Sec. IV. In Fig. 4 we plot these predicted masses as a function of the reduction scale factor. We see a marked change in the mass with reduced barriers. This may be associated with an increase in the yield of heavier fragments, as shown in Fig. 5. Considering these Coulomb effects we might expect that a freeze-out calculation would predict a lower mass for the final residue (or largest fragment) compared to the sequential calculation. The same difference in predictions is expected to occur if the effective freeze-out volume for the heavy fragments in a sequential calculation is smaller than the chosen freeze-out volume. This would also result in a relative suppression of the heavier fragments and hence a larger mass for the final residue.

The relative decrease in the Coulomb barrier in sequential decay effects not only the mass of the residue but also the proton-to-neutron ratio in that residue. Normal sequential decay barriers produce proton rich residues.

A reduced Coulomb barrier results in an increase in the mean multiplicity of charged particles as shown in Fig. 6. Thus, we might expect freeze-out calculations to predict higher charged-particle multiplicities than sequential decay calculations.

Finally, the Coulomb effects can influence the predicted distribution of isotopes of a given element. One would expect an enhancement in the yield of more neutron-rich isotopes for freeze-out calculations.

It should be noted that the reduced Coulomb barriers actually result in a larger fraction of the total excitation energy going into Coulomb-related kinetic energy. This is due to the increase in the yield of charged particles which more than compensates for the lower Coulomb energy for each fragment.

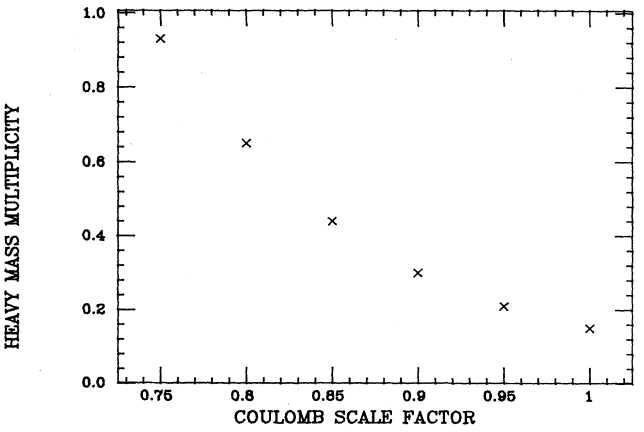

FIG. 5. Multiplicity of heavy fragments, from the decay of ^{197}Au excited to 538 MeV, as a function of the scale factor for the Coulomb barriers in sequential decay.

VI. SPECIFIC COMPARISON BETWEEN PREDICTIONS: DIFFERENCES

In this section we compare the results of two sets of predictions for the disassembly of the same system. The

calculations were made with two programs based on the two procedures discussed earlier. Our employed the procedures of Ref. 1, and the other employed the freeze-out procedures embodied in the formalism of Gross.[5] Each of these calculations has a myriad of detailed features which make highly quantitative comparisons difficult. The qualitative comparisons of the predictions, however, do illustrate many of the points discussed in earlier sections.

The system studied was ^{197}Au excited to an energy of 538 MeV. The radius chosen for the freeze-out volume was $r_0 = 2.05$ fm. The Fermi energy used in the emission program was 30 MeV. The two calculations have different collections of fragment masses. The emission program includes only systems with mass less than 20. The freeze-out calculation includes isotopes of masses up to the starting system. The mean value for the mass of the second heaviest fragment in the freeze-out calculation was 9.87, so it is unlikely that this difference will change the qualitative comparison. There are also some minor differences between the calculations in the number of the excited states which are included. In the following paragraphs we discuss specific predictions made by the two approaches and attempt to account for the differences in terms of the features discussed in previous sections. Among the predictions are (a) total multiplicity, (b) mean mass of the heaviest fragment (residue), (c) ratio of neutral (neutrons) to charged fragments, (d) the ratio of hydrogen isotopes, (e) the multiplicity of helium isotopes, and (f) the multiplicity of heavy fragments (mass greater than 8).

First we consider the mean multiplicity, not counting the final residue. The sequential calculation predicts 28 fragments including neutrons, while the freeze-out calculation predicts 24.5 fragments including neutrons. This can be understood in terms of the difference between the freeze-out volume and the effective volume associated with total multiplicity. The ratio of the two predictions is 1.14. When the sequential calculation was performed with Coulomb barriers scaled by factors of 0.9 and 0.8, we obtain mean multiplicities of 28 and 27, and corresponding ratios to the freeze-out predictions of 1.14 and 1.10, respectively. The ratios of the effective volume to the freeze-out volume are 1.707, 1.445, and 1.1086 for Coulomb barriers scaled by 1.0, 0.9, and 0.8, respectively. Thus, the ratio of predicted multiplicities can be understood in terms of the different effective volumes in conjunction with a Coulomb adjustment as discussed in Sec. V.

For the second comparison we consider the predicted mass of the final residue. In the freeze-out calculation, for which there is no "residue," we take the mean mass of the heaviest fragment. The calculation of Gross provides a mass of 140 for this in the test calculation. The prediction of the sequential decay model is for a mass of 156. If the Coulomb barrier is scaled by factors of 0.9 and 0.8, however, the predicted residue masses are 150.5 and 143.2, respectively. This would suggest that the mean mass of the heaviest fragment is sensitive to the mechanism that is involved in the fragmentation process. This difference is governed by the difference in the Coulomb effects between the two mechanisms.

As the next comparison let us consider the ratio of neutral (neutrons) to charged fragments (in addition to the residue). In these predictions we find large differences. The freeze-out calculation predicts 0.7713, while the sequential calculation predicts 3.26. The ratio of these predictions is 4.23. The effective volumes for the neutrons and the charged particles are different. For an normal Coulomb barrier the ratio of these volumes is 2.26. This is insufficient to account for the difference in predictions of the two procedures. If, however, we scale the Coulomb barrier by 0.9 and 0.8 the ratio of the ratios from sequential decay and freeze out drops from 4.23 (above) to 3.27 and 2.39, respectively. The ratio of neutral and charged effective volumes calculated for the two scaled Coulomb barriers are 2.38 and 2.40. We thus see that the differences can again be seen to be consistent with a combination of Coulomb and "volume" effects.

We next compare predictions for the relative yield of isotopes as predicted by the two methods of calculation. We concentrate on the isotopes of hydrogen. The freeze-out calculation provides d/p ratios of 1.77 and t/p ratios of 1.89. On the other hand, the sequential decay calculation provides, d/p ratios of 1.13 and t/p ratios of 0.680. If the Coulomb barrier is scaled by factors of 0.9 and 0.8, the ratios are 1.14 and 0.710 for the former and 1.18 and 0.777 for the latter. Clearly the sequential decay predictions are considerably less than the freeze-out predictions. In addition, the Coulomb effects are small, as one might anticipate.

We see that the ratio of the freeze-out d/p prediction and the sequential d/p prediction is 1.56. For this case the effective volumes for p and d differ primarily due to their mass difference, and the corresponding influence on their velocities. Calculation of the ratio of the effective volumes provides about 1.5, with small sensitivity to Coulomb scaling. Thus, the "volume" effects allows us to understand the difference in the d/p predictions.

The ratio of the t/p predictions from the freeze-out and from the sequential points of view gives 2.78. The calculated ratio of effective volumes for protons and tritons is about 1.9. While this large factor is qualitatively consistent with the ratio of predictions, it is not large enough to fully explain the differences. No obvious additional explanation has been found.

Let us next consider the predicted yield for the sum of helium isotopes of masses 4 and 5. The freeze-out calculation provides a multiplicity of 3.49 while the sequential decay calculation predicts 2.115. This represents a ratio of 1.65. The ratio of the freeze-out volume to the effective volume is 1.06. When we compare the predicted ratios with Coulomb barriers scaled by 0.9 and 0.8 we find 1.14 and 0.95 instead of 1.65 (full barrier). The corresponding ratios for the freeze-out volumes to the effective volumes are 1.15 and 1.36, respectively.

Finally let us compare the predictions for the multiplicity of fragments of mass greater than 8. Excluding the residue, the freeze-out calculation predicts a mean multiplicity of 0.44 particles for such particles. The sequential decay calculation predicts a multiplicity of only 0.15. Thus, the ratio of the predictions is 2.93. The ratio of the

effective volume to the freeze-out volume is 2.07 for the full Coulomb barrier. For Coulomb barriers scaled by 0.9 and 0.8, the multiplicity of the heavier fragments predicted by the sequential decay procedure is greatly enhanced reaching 0.30 and 0.65, respectively. Ratios of the freeze-out predictions to these values give 1.46 and 0.68, respectively. The corresponding ratios of the effective volume to the freeze-out volume are 2.3 and 2.6. In the case of the heavier fragments one encounters more significant effects associated with the excluded volumes in the detailed calculation of the freeze-out predictions. For that reason the volume ratios given above are upper limits. The differences between the two calculations are once again qualitatively provided by the Coulomb and "volume" considerations.

In the preceding discussion we have compared the detailed predictions for a number of features of the fragment yields. These have utilized two procedures, one based on the sequential decay picture and the other on the freeze-out picture. While the predictions are qualitatively similar we have noted several instances of differences on the order of a factor of 2 or 3. On the one hand, these differences offer possible signatures by which the two schemes may be differentiated by data. On the other hand, we have shown in each illustrative example how the differences can be qualitatively understood on the basis of two fundamental features: (a) the difference in the Coulomb effects between the two procedures, and (b) the difference between the freeze-out volume and the fragment-dependent effective volume in the sequential decay picture.

VII. CONCLUSIONS

We have compared the sequential decay and the freeze-out procedures for predicting yields in the disassembly of excited nuclear systems. To facilitate this we have reformulated the two methods in such a way as to allow for a comparison of the structure of the expressions in each.

This exercise pointed out the Coulomb differences between the methods. It also permitted the introduction of the concept of an *effective* volume which replaces the freeze-out volume when the sequential decay approach is used. We have shown that this volume includes, as factors, the cross section for absorption and fragment velocity, both of which only appear in the sequential decay approach. The effective volume is shown to be related to the conservation of entropy in the sequential decay picture.

The freeze-out volume represents a common space volume in which all of the fragments may simultaneously be found. The effective volume in the sequential decay picture is a phase-space volume assigned to each particle when it is emitted. In this case the particles do not exist in a single spacial volume. None the less, it is found that the effective volume for the sequential decay process may, under certain circumstances, be nearly equal in magnitude to typical freeze-out volumes. As such, the multiplicity predictions of the two procedures may be similar. This similarity arises even though the assumptions of the two procedures are mutually exclusive.

We have made a detailed comparison of two sets of predictions applied to the same system and have shown that the differences can be understood in terms of the volume differences and the Coulomb differences between the two points of view. The differences that we have examined offer an opportunity to differentiate between the underlying physical processes by examining, for example, masses and charges of the residue, neutron yields, charged-particle multiplicities, and the multiplicity of heavy fragments.

ACKNOWLEDGMENTS

The author wishes to gratefully acknowledge the warm hospitality of the Hahn-Meitner Institute of Berlin in 1988 where this work was begun with the stimulating and invaluable aid of Prof. D. H. E. Gross, and with many very useful conversations with Dr. K. Möhring, Dr. B. Hiller, and Dr. A. Blin. This work was supported in part by a grant from the National Science Foundation.

*Permanent address: Physics Department, University of Wisconsin, Madison, WI 53706.

[1]W. A. Friedman and W. G. Lynch, Phys. Rev. C **28**, 16 (1983).
[2]V. F. Weisskopf, Phys. Rev. **52**, 295 (1937).
[3]D. H. E. Gross, X. Z. Zhang, and S. Y. Xu, Phys. Rev. Lett. **56**, 1544 (1986); X. Z. Zhang, D. H. E. Gross, S. Y. Xu, and Y. M. Zheng, Nucl. Phys. **A461**, 668 (1987).
[4]W. A. Friedman, Ann. Phys. (N.Y.) **192**, 146 (1989).
[5]D. H. E. Gross (private communication).